JOURNAL OF GEOPHYSICAL RESEARCH, VOL. 91, NO. B8, PAGES 8113–8125, JULY 10, 1986

Orientation, Relative Age, and Extent of the Tharsis Plateau Ridge System

THOMAS R. WATTERS AND TED A. MAXWELL

Center for Earth and Planetary Studies, National Air and Space Museum, Smithsonian Institution, Washington, D. C.

The Tharsis ridge system is roughly circumferential to the regional topographic high of northern Syria Planum and the major Tharsis volcanoes. However, many of the ridges have orientations that deviate from the regional trends. Normals to vector means of ridge orientations, calculated in 10° boxes of latitude and longitude, show that the Tharsis ridges are not purely circumferential. Intersections of vector mean orientations plotted as great circles on a stereographic net show that the ridges are not concentric to a single point but to three broad zones. These data indicate either that the Tharsis ridge system did not form in response to a single regional compressional event with a single stress center or that the majority of the ridge system did form in a single event but with locally controlled deflections in the generally radially oriented stress field. Superposition relationships and relative ages suggest that the compressional stresses that produced the ridges occurred after the emplacement of the ridged plains volcanic units (early in the Hesperian period) but did not extend beyond the time of emplacement of the Syria Planum Formation units or the basal units of the Tharsis Montes Formation (during the latter half of the Hesperian period). Comparison of topographic data with the locations of ridges demonstrates a good correlation between the topographic edge of the Tharsis rise and outer extent of ridge occurrence. Compressional deformation related to Tharsis is present out to about 5100 km from the regional topographic center located near northern Syria Planum. The innermost extent cannot be determined because the ridged plains units have been buried by more recent volcanic units, although ridge formation appears to have extended farther inward than is presently observed. Models involving a combination of isostatic stresses and stresses resulting from flexural loading appear to explain best the observed tensional features, topography, gravity, and, to a first approximation, the locations and orientations of the compressional ridges.

INTRODUCTION

The Tharsis Plateau of Mars is one of the most extensive volcanic and tectonic regions known on the terrestrial planets. The plateau is characterized by a broad topographic rise and dominated by the large shield volcanoes, Olympus, Arsia, Pavonis, and Ascraeus mons. The major structural features of the Tharsis Plateau are a radial fracture system extending over approximately 25% of the surface of the planet [*Wise et al.*, 1979] and a circumferentially oriented ridge system. Tharsis ridges range from 2 to 6 km wide and extend from 50 to 150 km long. These ridges occur within, and in some areas beyond, the radial fracture zone on relatively smooth volcanic plains units that have flooded older and more densely faulted cratered terrain. The ridged plains units have been faulted but to a much lesser degree than the older cratered terrain. These ridges may be (1) folds formed by regional or local compressional stress [*Watters and Maxwell*, 1983, 1985*a*], (2) the surface manifestation of reverse or thrust faults [*Plescia and Golombek*, 1985], or (3) folds with thrust faulting developing as a result of fold geometry [*Watters and Maxwell*, 1985*b*].

The Tharsis Plateau is characterized by a large positive free air gravity anomaly [*Phillips et al.*, 1973; *Phillips and Saunders*, 1975; *Balmino et al.*, 1982]. Applying an isostatic compensation mechanism for the gravity data (Bouguer gravity minus the gravity due to the root) results in a positive residual anomaly over the plateau [*Phillips et al.*, 1973; *Phillips and Saunders*, 1975].

The purpose of this study is to investigate (1) the orientations of the Tharsis Plateau ridge system and the symmetry of the inferred compressive stress field, (2) the relative ages of the compressional events that generated the ridges, and (3) the extent of Tharsis-related compressional deformation. In addition, models for the origin of stresses in the Tharsis region are investigated in relation to the formation of the ridges.

Paper number 5B5746.
0148-0227/86/005B-5746$05.00

RECENT STUDIES

In a comprehensive tectonic study of the Tharsis region, *Wise et al.* [1979] present a model of an early topographic rise, followed by extensive, long-lived volcanism. Analysis of stereographic plots of fractures and ridges mapped primarily from Mariner 9 and early Viking orbiter images confirmed a predominantly radial orientation of the faults and a circumferential arrangement of ridges. Based on crater ages, they suggested that the ridges were approximately coeval with the main radial fault system. Deviations from Tharsis-related orientations were attributed to a NE trending crustal anisotropy related to the boundary between the highlands and the lowlands, parallel to the line of the Tharsis volcanoes.

In studies of the ridged plains units of Coprates and Lunae Planum, *Saunders and Gregory* [1980], *Saunders et al.* [1981], and *Watters and Maxwell* [1985*a*] suggest that the regularity of the ridge spacing was controlled by a dominant wavelength of folding. An alternative control may be preexisting basement faults, although ridge orientations are not similar to those of the surrounding fault systems [*Maxwell*, 1982]. In a study of the Tharsis fault system, *Plescia and Saunders* [1982] present a model involving several discrete episodes of uplift and faulting. According to their model the earliest tectonic activity, located in the Thaumasia region,

Fig. 1. Ridges in the western hemisphere of Mars. Ridges form a small circle centered roughly on Pavonis Mons. The largest number of ridges occur on the ridged plains east of the major Tharsis volcanoes in the Coprates and Lunae Planum regions. This projection is centered at 0°N, 110°W and represents 1853 digitized segments (Apt represents volcanic plains of Tharsis Montes region [*Scott and Carr*, 1978]).

was followed by faulting centered on northern Syria Planum and then by two more episodes of faulting, both centered near Pavonis Mons. They suggest that the ridges in the Tharsis region formed late in the tectonic history of the province and that the ridges represent a viscoelastic response of the lithosphere to the Tharsis load.

Watters and Maxwell [1983] present the results of observations of the ridge-fault crosscutting relations in the Tharsis region and suggest a classification system involving three distinct types of ridge-fault intersections: ridges crosscut by faults, superposed by faults, and terminated at one end by faults. Relative age relationships based on these intersection types indicate that ridges were formed both before and after extensional faulting. Using ridge-fault crosscutting relations and the angle of intersection between ridges and Tharsis radial faults, *Watters and Maxwell* [1983] conclude that the major ridge-forming events in the Tharsis region were roughly coincident with, and in many cases prior to, the extensional events that produced the faulting of the Tempe Terra, Coprates, and Memnonia regions and the rifting of Valles Marineris.

Geophysical studies of the tectonic evolution of the Tharsis region have focused on the relative role of stresses generated from isostatically compensated uplift versus flexural load, using the Tharsis fault system as the major constraint [*Solomon and Head*, 1982; *Willemann and Turcotte*, 1982; *Banerdt et al.*, 1982; *Sleep and Phillips*, 1985]. This has resulted in a controversy over which mechanism dominated in the tectonic evolution of Tharsis. Relatively few geophysical studies have addressed the origin of the Tharsis ridge system or its significance to the tectonic history of the region.

Results

Orientations of the Ridge System

The ridge system of Tharsis is approximately circumferential to the regional topographic high in northern Syria Planum and the major Tharsis volcanoes (Figure 1). These ridges are interpreted as compressional features that formed in response to a radially oriented stress field with a center near the Pavonis Mons volcano, assuming that the maximum principal compressive stress σ_1 was perpendicular to the long axes of the ridges.

Our data permit a detailed analysis of the orientations of the Tharsis ridges. Normals to vector means of ridge orientations were calculated using the over 1850 digitized ridge segments sampled in 10° boxes of latitude and longitude (Figure 2). The ridges were digitized from U.S. Geological Survey (USGS) 1:2,000,000 Mercator and Lambert projection controlled orthophoto maps. Due to resolution limits, individual segments of less than 5 km length were merged with longer ridge segments or omitted. Orientations of individual ridge segments were determined and weighted by length, and mean orientations or vector means were then computed [see *Reiche*, 1938]. The magnitude of each result-

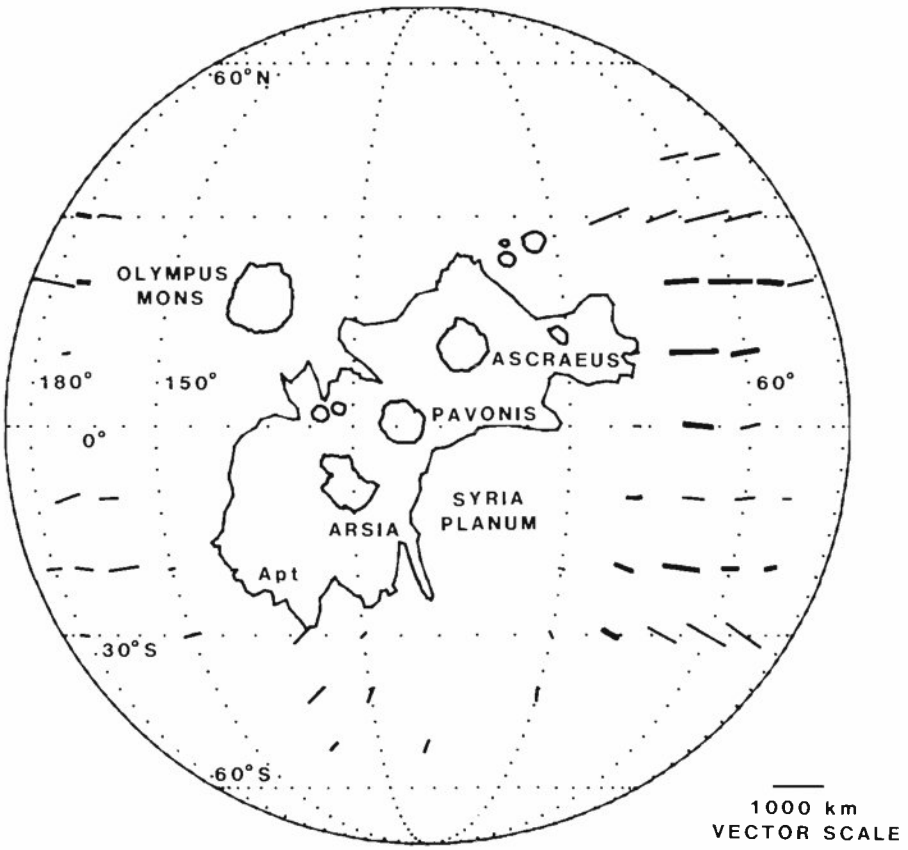

Fig. 2. Normals to vector means using 1853 digitized ridge segments sampled in 10° boxes. Orientations of individual ridge segments were weighted by lengths to determine vector means. Line lengths shown are weighted by vector magnitude, with double width lines representing 4× the magnitude of single thickness lines. Normals to vector means with magnitudes less than 100 km are not shown. This projection is centered at 0°N, 110°W.

ant vector mean was weighted by the total length of the ridge segments within the given 10° box and normals to the vector means were then determined (Figure 2). Normals to vector means with magnitudes less than 100 km were considered to be insignificant and were not included in the analysis. The resulting vectors are inferred to represent the average regional maximum compressive stress vectors of the stress field that generated the ridges in the Tharsis region. The average compressive stress orientations around Tharsis indicate that the ridge system is not concentric to any single point.

In order to evaluate further the radial symmetry of the inferred stress field, vector mean orientations were plotted as great circles on the upper hemisphere of a Schmidt equal-area stereographic net. Concentrations of 1225 intersections of the great circles were determined and contoured (Figure 3). This analysis indicates that the inferred stress field is radial to three broad zones centered (1) southwest of Olympus Mons, (2) north of Lunae Planum, and (3) on Syria Planum. In contrast to the findings of *Wise et al.* [1979], the greatest concentration of intersections occurs in the Syria Planum region at approximately 17°S, 105°W rather than west of the Tharsis Montes volcanic line. The lack of radial symmetry of the inferred stress field may be explained in two ways: (1) the system formed in two or more distinct events with different stress fields and centers, or (2) a single, radially oriented stress field was deflected due to locally controlled influences.

The vector mean analysis of the ridge system also indicates the relative magnitude of the compressive strain since the resultant vector is length weighted by the total number of ridge segments within the sampled areas. The results suggest that the distribution of compressive strain on the exposed ridged plains units is not uniform (Figure 2). However, since the areal extent of ridged plains units is also not uniform, large differences in the observed vector magnitudes are in many cases the results of differential exposure of plains material.

Relative Age of Ridge Formation

The relative age of the ridge-forming events in the Tharsis region can be constrained by superposition relationships of the units on which the ridges occur. Since the majority of the stratigraphic units in the Tharsis region are volcanic, superposition relationships can be determined by photogeologic interpretation of the volcanic flow units using Viking orbiter images.

Units in the Coprates region, located on the southeastern portion of the Tharsis Plateau, are well exposed. Here ridge orientations vary from a strong NE trend in southwestern Coprates to N-NE in northwestern Coprates (A and B in Figure 4). In southwestern Coprates, three distinct units can be easily delineated by means of superposition relations and crater density [*Scott and Tanaka*, 1984] (Figure 5). From oldest to youngest these are heavily cratered and faulted upland (Nb) delineated by numerous N-S and NW trending

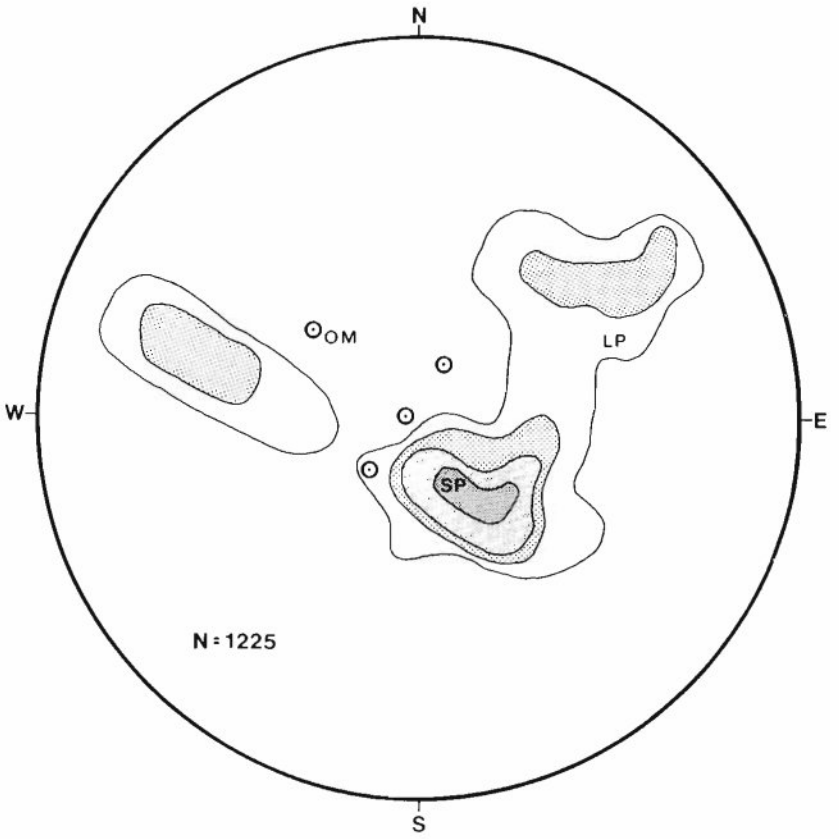

Fig. 3. Density of intersections of vector mean orientations plotted as great circles on the upper hemisphere of a Schmidt equal-area stereographic net. Concentrations of 1225 intersections were determined using a Kalsbeek counting net. Contours represent 1–2–3–4% per 1% area. Maximum concentration is located in Syria Planum at approximately 17°S, 105°W. This projection is centered at 0°N, 110°W.

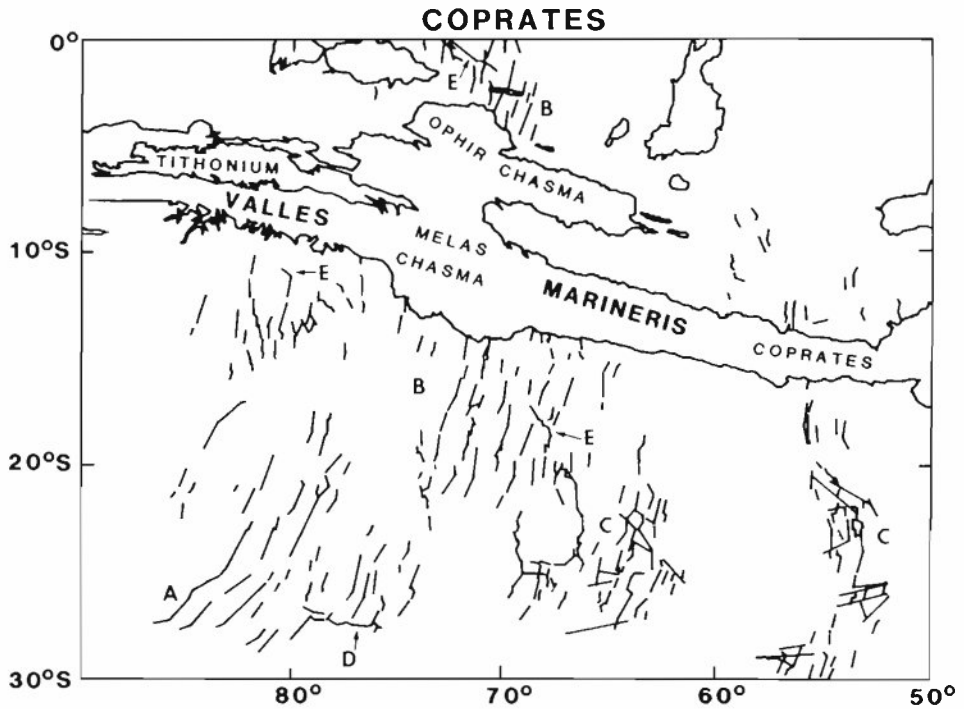

Fig. 4. Ridges in the Coprates region. Ridge orientations vary from NE trends in SW Coprates (A) to N-NE in NW Coprates (B). In south central and SE Coprates, N-NE to N-NW trending ridges are superposed by W-SW and W-NW trending ridges (C) described by *Saunders et al.* [1981] as reticulate patterns. A small number of E-W trending ridges occur in SW Coprates (D). Isolated NW trending ridges occur in central and NW Coprates (E).

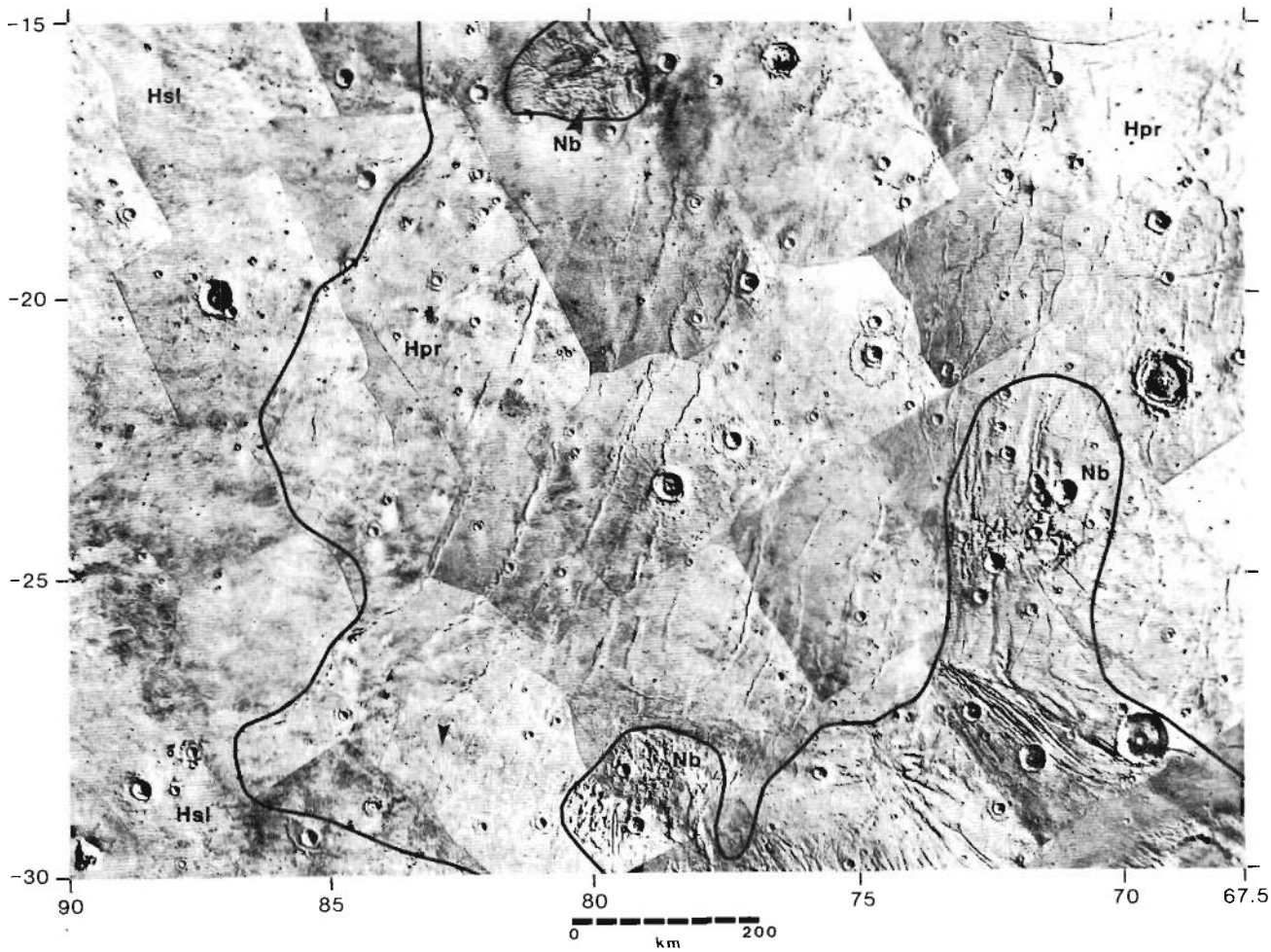

Fig. 5. Geologic units of southwest Coprates. Hsl represents the Syria Planum flow unit [*Scott and Tanaka*, 1984]; Hpr represents the ridged plains unit [*Scott and Tanaka*, 1984]; Nb represents basement complex commonly intensely cratered [*Scott and Tanaka*, 1984]. Base map is USGS 1:2,000,000 controlled photomosaic of SW Coprates (MC-18 SW).

faults; ridged plains (Hpr) characterized by curvilinear ridges with a predominantly N-NE trend which exhibit regular spacing; and smooth plains (Hsl) delineated by well-defined flows. The faults delineating the faulted upland terminate sharply at the contact with the ridged plains units. At the contact between the smooth plains and the ridged plains, volcanic flow fronts are present and extend into the interridge plains, partially to completely burying some ridges (Figure 6). Comparison of ridge elevations of partially buried ridges on the western edge of the ridged plains unit with those in central and southwestern Coprates suggest that flows superposed on the interridge plains do not exceed a few hundred meters in thickness. The morphological relationships between the ridges and the flow fronts indicate that the formation of the ridges predates the emplacement of the volcanic flow units of the smooth plains.

Cross sections of this area were constructed using topographic profiles derived from earth-based radar altimetry data [*Roth et al.*, 1980]. The observed topography may be due to uplift of the volcanic sequence (Figure 7*a*) or to westward thickening of Syria Planum flow units with no uplift (Figure 7*b*). The ridged plains unit is probably underlain by a regolith of unconsolidated impact breccias, with or without intermixed pyroclastics. The existence of an unconsolidated regolith unit is inferred from debris flows emanating from some areas of the walls of Valles Marineris. The regolith overlies highly cratered basement units (Terra Material, HNht of *Scott* [1981]; or Basement Complex, Nb of *Scott and Tanaka* [1984]) which are ancient crustal materials and probably the oldest exposed units on the planet [*Scott*, 1981].

A similar stratigraphy is present to the north of Coprates in the Tempe Terra region (Figure 8). Ridges in the Tempe Terra region have a predominantly NW trend and occur as close as 20 km to the contact between the ridged plains unit and a member of the Tharsis Formation (Ht_2, Tharsis Formation of *Scott and Tanaka* [1984]). The distinctive flow fronts characteristic of the Syria Planum flow units in southwestern Coprates are absent in the Tharsis Formation flows in the Tempe Terra region. The numerous NE and N-NE trending faults that clearly cut the ridged plains units of Tempe are buried by the Tharsis Formation (Figure 8), and only a few younger NE trending faults cut both the Tharsis Formation and the ridged plains. In addition to the abrupt termination of the faults, no ridges are present on the Tharsis Formation (Ht_2).

The most significant of these observations is that no ridges are present on any stratigraphically younger units than the

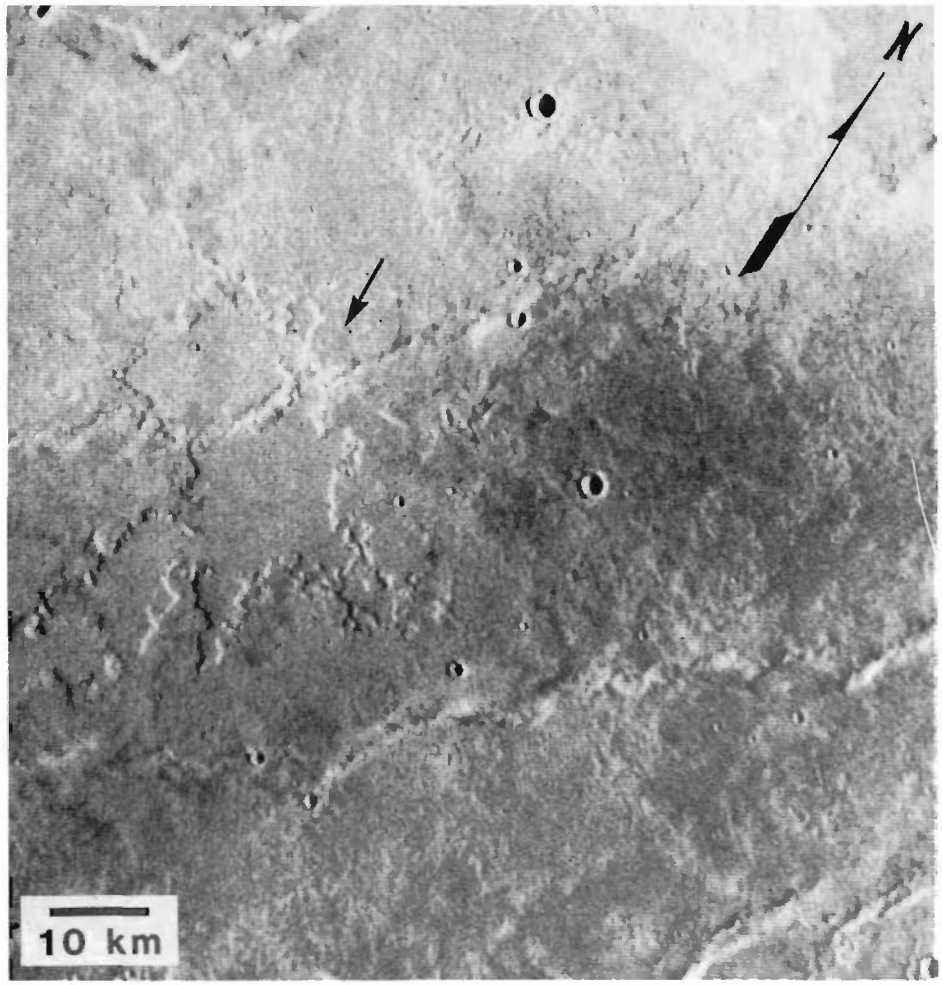

Fig. 6. Digitally enhanced Viking orbiter image of a volcanic flow in the interridge plains that has completely engulfed a ridge in southwestern Coprates (Viking orbiter frame 608A22). Only a small portion of the ridge crest remains exposed. The relationship between the flow front and the ridge suggests that the flow postdates the ridge.

ridged plains units in the Tharsis region (excluding those ridges in the Olympus Mons caldera reported by *Lucchitta and Klockenbrink* [1981]). This implies that the ridges formed after the emplacement of the ridged plains volcanic units but before the emplacement of the Syria Planum flows, the Tharsis Formation flows, or any other stratigraphically younger unit on the Tharsis Plateau.

Further support for this timing of ridge formation is given by recently completed mapping and crater counts of the geologic units in the western equatorial region of Mars by *Scott and Tanaka* [1984]. Their data support the conclusions that compressional ridges are confined to plains units that were emplaced on the heavily cratered basement unit and that ridge formation did not extend to stratigraphically younger flow units.

Areal Extent of Compressional Deformation

The extent of Tharsis-related compressional deformation is important in trying to understand the nature of the ridge-forming events in the Tharsis region. Determination of the distal limit of ridge formation is relatively straightforward for most of the region since, beyond a certain distance from an arbitrary point near the center of the Tharsis rise, the number of ridges diminishes. In many areas of the Tharsis Plateau the locations where ridge formation appears to have attenuated is at or near the topographic boundary of the rise (Figure 9).

Two areas where this relationship is not clear are Chryse Planitia and Amazonis Planitia. Both of these regions border Tharsis and both are topographic basins distinct from the Tharsis Plateau. Deviations from regional trends in these areas may be the result of stresses generated within these basins coupled with Tharsis-related compressional stress.

To evaluate the extent of ridge formation, the frequency of ridge segments per radius increment and total length of ridge segments per radius increment are plotted as a function of distance from the topographic center. Ridges occur from 1100 to 5100 km from the regional topographic center near northern Syria Planum (7°S, 103°W); frequency and total length peaks at 2600 and 2500 km, respectively (Figure 10). Northern Syria Planum is chosen as a reference point because it is both the approximate topographic center of the plateau and also the highest point of the Tharsis rise excluding the major volcanoes [see *Downs et al.*, 1982].

Because average ridge spacing remains relatively constant over most of the ridged plains (Hpr) [see *Saunders and Gregory*, 1980], the peaks of ridge distribution (which corresponds to central Coprates and Lunae Planum) may be interpreted as representing the areas of maximum compressional deformation in the Tharsis region. However, because

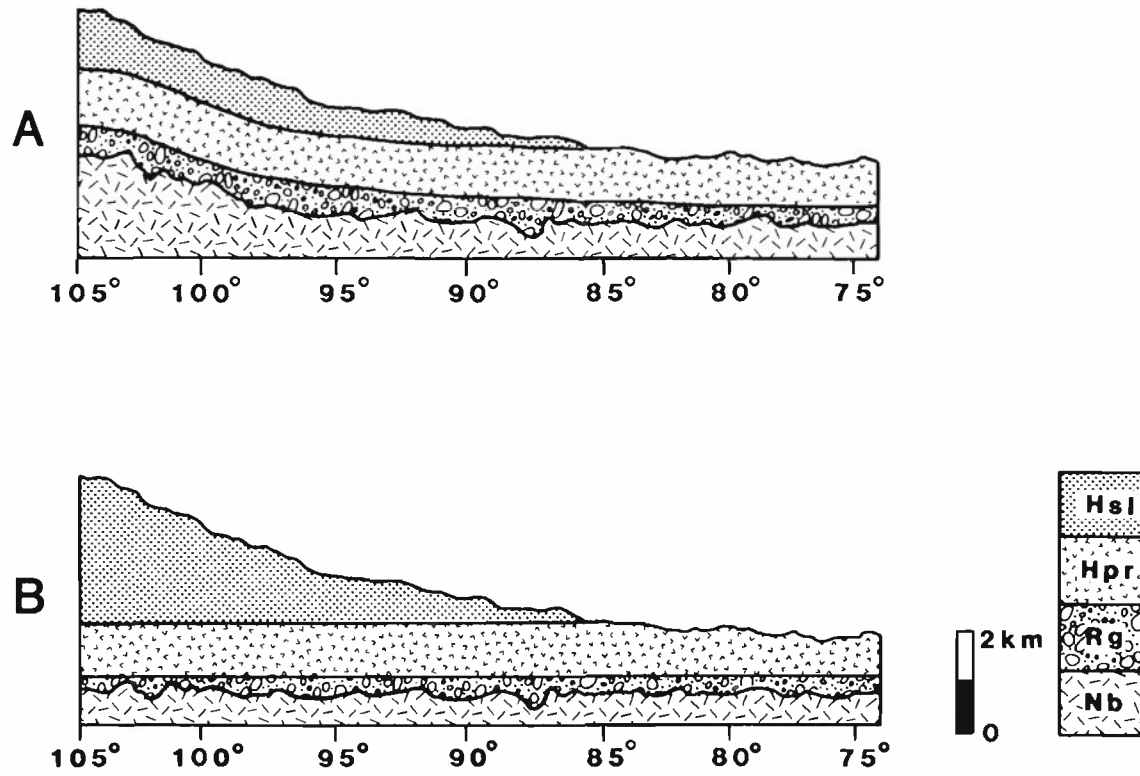

Fig. 7. Hypothetical cross sections of the Syria Planum–southwest Coprates region along 20°S latitude (see Figure 4). Topographic profiles are based on radar altimetry data [*Roth et al.*, 1980]. Cross sections represent the topography and units for two models. (*a*) Uplift of the volcanic sequence centered in the Syria Planum region. (*b*) Volcanic pile with no uplift. Hsl is Syria Planum flow unit, Hpr is ridged plains unit, Rg is a regolith unit, and Nb is Basement Complex. The thickness of the regolith is not constrained.

the distribution of ridged plains units is not uniform on the plateau, the peaks in the frequency versus distance plot are heavily biased by the fact that Coprates and Lunae Planum have the largest continuous exposure of the ridged plains.

Although it is possible to assess the outermost extent of Tharsis-related compression, the inner extent cannot be similarly determined because the ridges have been buried by volcanic flows. The partially buried ridges of western Coprates, 1100 km from the center, represent the innermost observable extent of compression. The sharp decrease in total ridge lengths between western Coprates and northwestern Lunae Planum probably reflects the extent to which ridged plains have been buried by recent volcanic flows or obscured by other resurfacing processes (Figure 10). Consequently, the observed ridges may represent only a fraction of the total compressional deformation that occurred on the ridged plains units.

Discussion

Major Tectonic Events

Based on superposition relationships presented in this study, crater density numbers from *Scott and Tanaka* [1984], and a study of the evolution of the Tharsis fault system by *Plescia and Saunders* [1982], the major tectonic events in the Tharsis region can be summarized (Figure 11). The geologic history of the western equatorial region is divided into three periods which are, from oldest to youngest, (1) the Noachian period, (2) the Hesperian period, and (3) the Amazonian period [*Scott and Tanaka*, 1984].

Tectonic activity in the Tharsis region appears to have started with the uplift of the Tharsis Plateau in the Noachian period (Figure 11), based on the high degree of faulting of the oldest exposed unit in the Tharsis region (Basement Complex). This period of extension generated the intense faulting in the Thausmasia highland, which may be the oldest regional fault system on the planet [*Plescia and Saunders*, 1982].

The beginning of the Hesperian period was characterized by the onset of plateau volcanism [*Scott and Tanaka*, 1984]. The ridged plains units were emplaced after the faulting of the Basement Complex (Figure 11). The source fissures or dikes of the ridged plains volcanic units are not known but are presumed to be near the center of the Tharsis Plateau because this is the source of all the more recent volcanic flow units. The emplacement of the ridged plains units was roughly coincident with another period of intense faulting recorded in units in northern Syria Planum, north of Noctis Labyrinthus, and Thaumasia [*Scott and Tanaka*, 1984]. These faults correspond to the Syria Planum–centered faults proposed by *Plescia and Saunders* [1982].

Superposition relations indicate that ridge formation began after the emplacement of the ridged plains. Based on ridge-fault crosscutting relations [*Watters and Maxwell*, 1983], ridge formation had generally ended when another period of faulting began. It was during this period of faulting that the majority of ridge-fault crosscutting relationships on the ridged plains were formed. This tectonic episode generated the faults in Coprates, Tempe Terra, Thaumasia, Phaethontis, and Memnonia that are approximately radial to

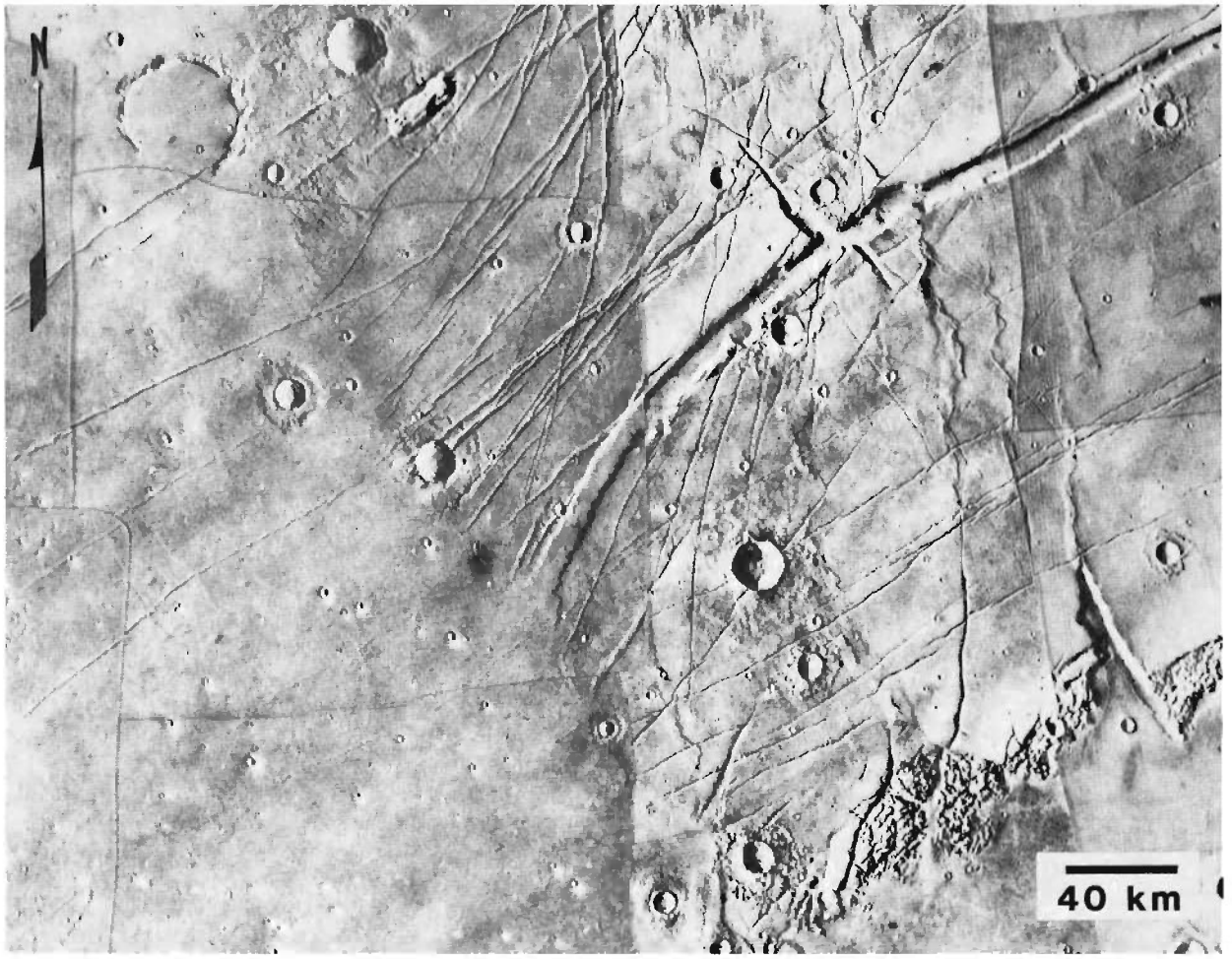

Fig. 8. Tempe Terra region showing the contact between the ridged plains unit (on the right) and a lower member of the Tharsis Formation (left). Ridges occur as close as 20 km from the contact between the two units (lower center). This figure is an enlargement of the USGS 1:2 000 000 controlled photomosaic of NW Lunae Planum (MC-10 NW).

a point near Pavonis Mons and are generally equivalent to the Pavonis I fault center proposed by *Plescia and Saunders* [1982].

The initial rifting of Valles Marineris also took place during the Hesperian period, as determined from crosscutting relations and intersections of ridges with the walls of Valles Marineris and related grabens [*Watters and Maxwell*, 1983]. These extensional events were followed by a major episode of erosion that dissected portions of the ridged plains of northern Lunae Planum and Tempe Terra, forming large channels and scarps, and eroded the interridge plains of Chryse Planitia. The steep scarps that mark the western edge of the ridged plains of Lunae Planum were formed by this erosional event [*Scott and Tanaka*, 1984].

This period of erosion was followed by another episode of widespread volcanism in the Hesperian period [*Scott and Tanaka*, 1984] which included (1) the Tharsis Montes flows that cover part of the ridged plains in Tempe Terra, Phaethontis, and Memnonia, (2) Syria Planum flows that cover part of the ridged plains in Coprates, and (3) the Alba Patera flows. The stratigraphic relations in southwest Coprates and Tempe Terra indicate that ridge formation did not continue after the onset of Syria Planum or Tharsis Montes–centered volcanism. The Tharsis Montes and Alba Patera–centered volcanism continued into the Amazonian period, while the Syria Planum centered volcanism ended in the later part of the Hesperian.

Following the decline of volcanic activity in the Amazonian period, a final extensional episode generated faults in the Tharsis Montes Formation, some of which extend onto the ridged plains of the Tempe Terra region. The NE trending faults that cut both the Tharsis Montes Formation and the ridged plains of Tempe were formed during this period. This period of extension corresponds to the Pavonis II–centered faulting episode of *Plescia and Saunders* [1982].

Models for the Origin of the Stresses

A number of models have been proposed to explain the origin of the stresses responsible for the tectonic features in the Tharsis region. These models involve three basic concepts: (1) loading of the crust, (2) isostatically compensated uplift, and (3) a combination of isostatically compensated uplift and loading.

Solomon and Head [1982] suggest that the Tharsis rise is purely a volcanic construct and that the regional fracture system resulted from load-induced stresses. *Willemann and Turcotte* [1982], like *Phillips and Golombek* [1983], believe that the contribution of the surface volcanic sequence to lithospheric loading is minor compared to the contribution by shallow igneous intrusives. Generally, these models have

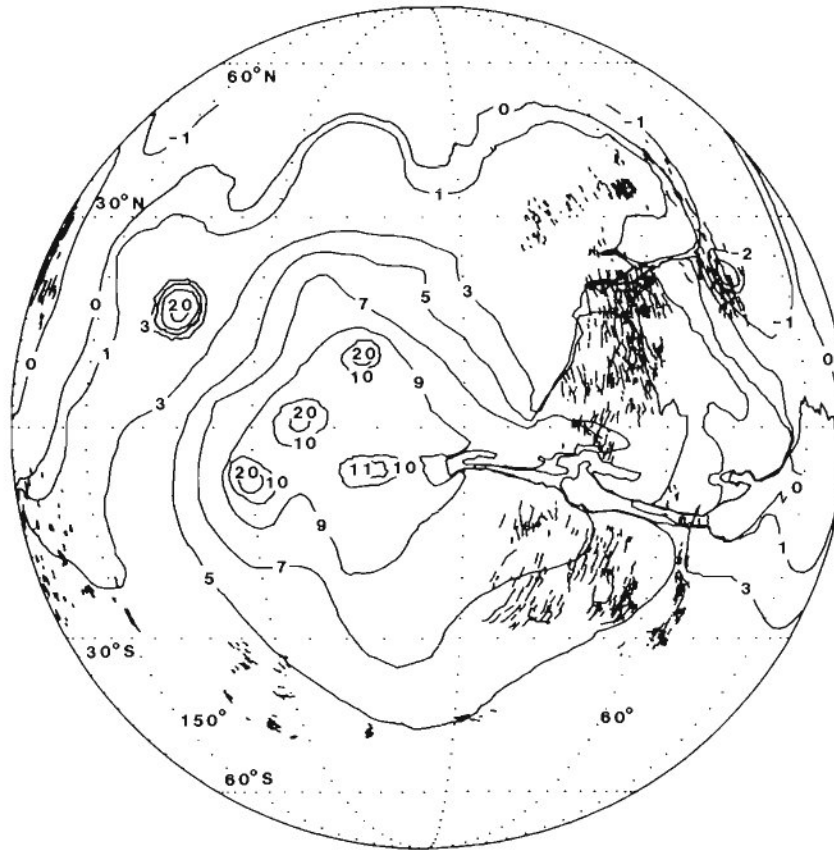

Fig. 9. Topography of the western hemisphere of Mars superimposed on the Tharsis ridge system. Note the correlation between the outermost occurrence of ridges and the present edge of the Tharsis rise. The major trends of the ridge system parallel the regional slope, as indicated by contour lines [from *U.S. Geological Survey*, 1976]. The topographic high point, less the Tharsis volcanoes, is located in northern Syria Planum, and the low point is located in Chryse Planitia. Contour lines represent altitude (in kilometers) relative to the 6.1-mbar atmospheric pressure surface. This projection is centered at 0°N, 95°W.

little to say concerning the formation of the compressional ridges except to suggest that they formed as a result of a long-term viscoelastic response of the lithosphere to the Tharsis load. This mechanism is not supported by the crosscutting relationship between the ridges and the radial grabens [*Watters and Maxwell*, 1983] or by the relative age of the volcanic plains units on which the ridges formed.

Models suggesting uplift [*Carr*, 1973; *Phillips et al.*, 1973; *Hartmann*, 1973; *Carr*, 1974; *Phillips and Saunders*, 1975; *Wise et al.*, 1979] involve domal uplift of the crust with

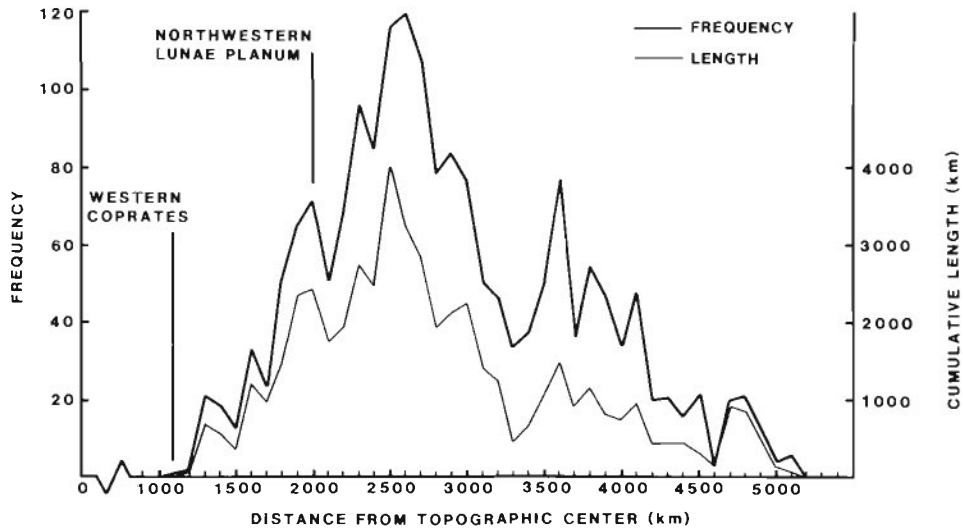

Fig. 10. Histogram plot of frequency and total length of ridge segments per radius increment as a function of distance from the regional topographic center (7°S, 103°W). Peaks at 2600 km and 2500 km of the frequency and total length, respectively, reflect maximum ridge densities in central Coprates and Lunae Planum.

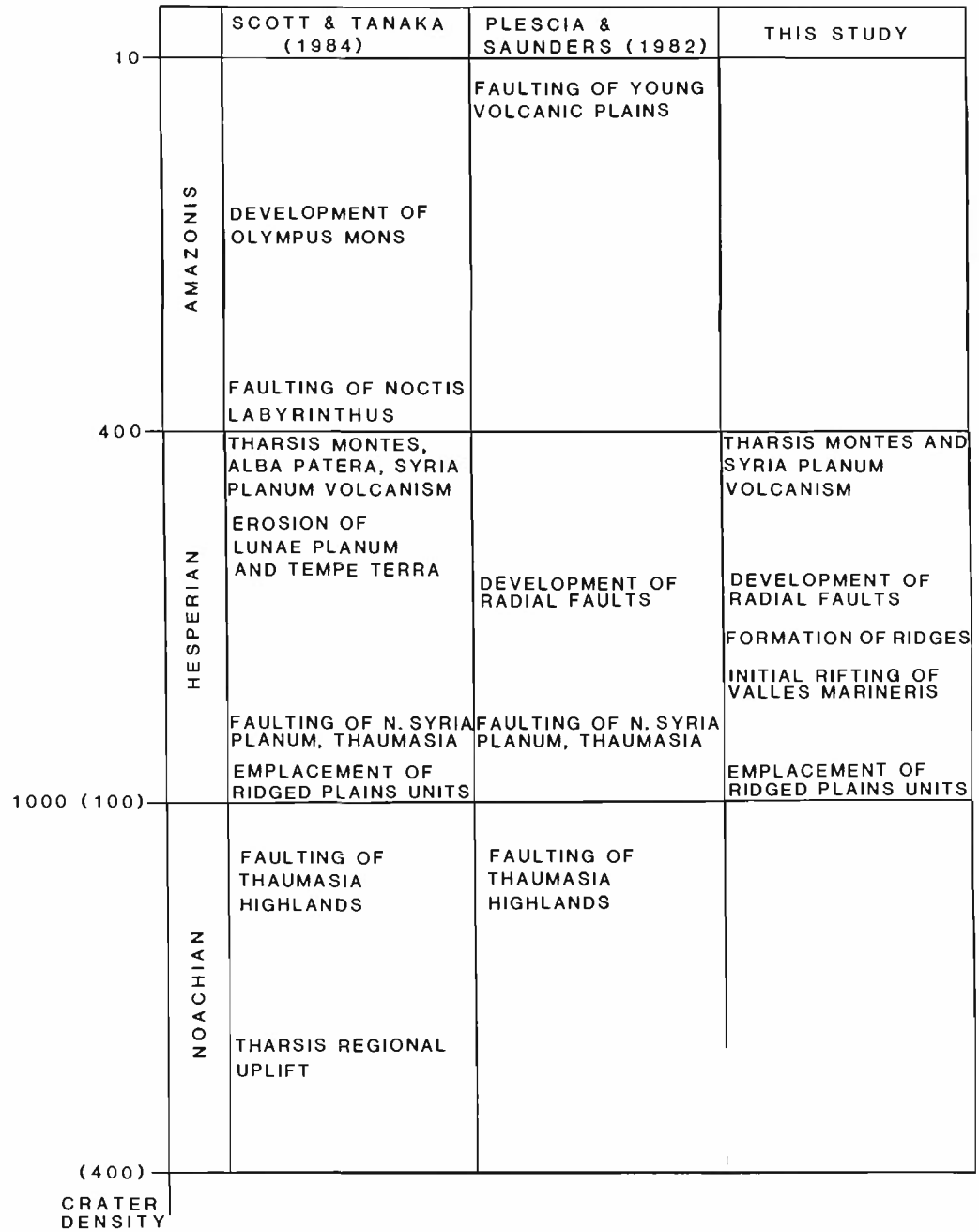

Fig. 11. Major tectonic events of the Tharsis region during the Noachian, the Hesperian, and the Amazonian periods. This sequence of events is based in part on superposition relations of the units and crosscutting relations between the ridges and faults and from data of *Scott and Tanaka* [1984] and *Plescia and Saunders* [1982]. Crater density ranges assigned to the geologic periods are from *Scott and Tanaka* [1984] (crater numbers in parentheses are for craters >16 km per 10^6 km^2 and numbers outside parentheses are for craters >2 km per 10^6 km^2). The structural events shown here are ordered with respect to their relative age only and cannot be directly affixed to the crater density scale.

associated fracturing of the lithosphere and formation of a radial graben system. The source of the uplift varies from thermal anomalies, a mantle plume, and convective upwelling of the mantle to changes in mantle phase chemistry.

Two models involving a combination of isostatic uplift and flexural loading have been recently proposed by *Banerdt et al.* [1982] and *Sleep and Phillips* [1985]. *Banerdt et al.* [1982] calculate the stress state in a thick lithosphere for three models: (1) isostatically compensated Tharsis topography, (2) topographic flexural loading of the lithosphere, and (3) flexural uplift of the lithosphere due to buoyant forces. In the flexural uplift model, the current Tharsis topography is caused by flexural doming of the lithosphere as a result of upward forces. Based on the poor correlation with extensional features, *Banerdt et al.* [1982] conclude either that flexural uplift was not an important mechanism in the tectonic history of Tharsis or that evidence of such an event has been obscured by more recent events. Calculated compressional stress trajectories for this model do not agree with the observed locations and orientations of the ridges [see *Banerdt et al.*, 1982, Figure 3*a*].

The stress calculations of *Banerdt et al.* [1982] for an

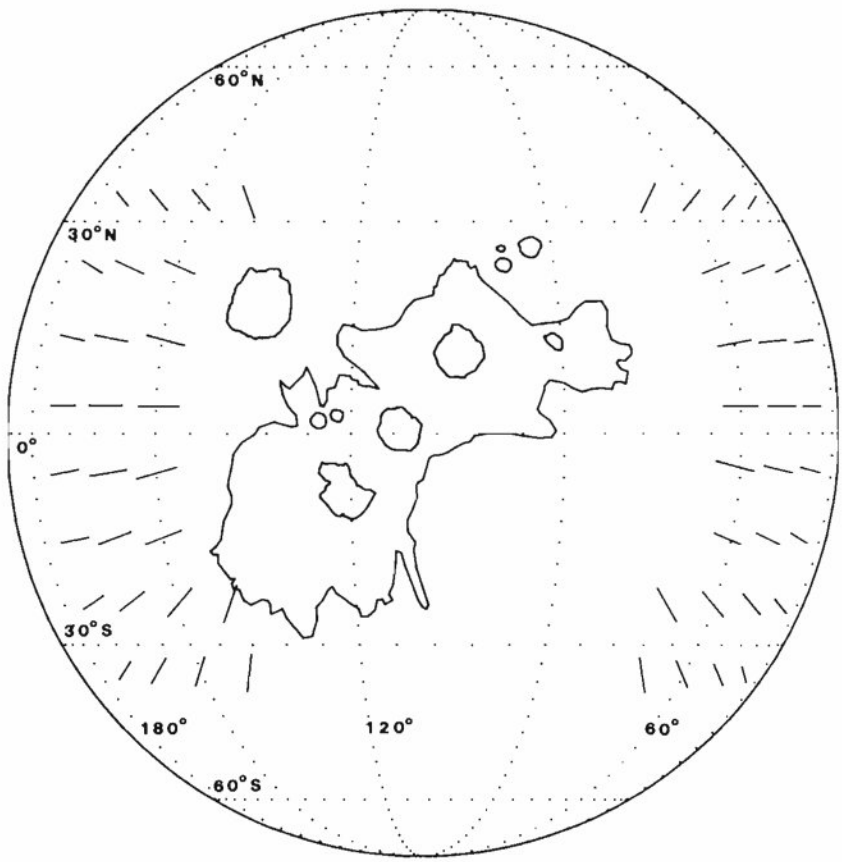

Fig. 12. Predicted compressional stress trajectories for the western hemisphere of Mars from *Banerdt et al.* [1982, Figure 3*b*], isostatic model plotted on a spherical projection. The locations and orientations of the isostatic stresses calculated by *Banerdt et al.* [1982] are very similar to those calculated by *Sleep and Phillips* [1985] [see *Banerdt et al.*, 1982, Figure 3*b*; *Sleep and Phillips*, 1985, Figure 2]. This projection is centered at 0°N, 110°W.

isostatically compensated Tharsis use the models of *Sleep and Phillips* [1979] and *Finnerty and Phillips* [1981]. Predicted tensional stresses agree well with the central Tharsis faults, out to a radius of 40° or about 2200 km from the center of Tharsis [see *Banerdt et al.*, 1982, Figure 3*b*]. Beyond 2200 km from their center (located near 5°N, 107°W), the isostatic model predicts stresses that are dominantly compressive (Figure 12). Their calculated stress trajectories indicate a largely radially oriented compressional stress field that roughly approximates the observed orientations and locations of the inferred stresses (compare Figure 2 with Figure 12). The correlation between the predicted and inferred stresses is weakest in the Memnonia region and is limited to areas where the ridged plains units are exposed.

Stress trajectories obtained from a flexural loading model predict a circumferentially oriented tensile stress field beyond 40° (or 2200 km) that agrees well with the observed outer radial fault system of Tharsis (also see *Golombek and Phillips* [1983]). The isostatic and flexural loading models are complimentary in the sense that they predict tensional and compressional features that are orthogonal.

Sleep and Phillips [1985] propose a model for isostatic compensation in one-plate planets which accounts for membrane stresses in the lithosphere, rotational ellipticity, and self gravitation. They calculate the lithospheric stresses resulting from isostatic compensation and flexural loading on Mars. The locations and orientations of tensional and compressional stresses for the isostatic and flexural loading models of *Sleep and Phillips* [1985] are very similar to the isostatic and flexural load models of *Banerdt et al.* [1982]. Both calculate stresses that are radially compressive in the center of Tharsis for the flexural model and radially compressive in outer Tharsis for the isostatic model. *Sleep and Phillips* [1985] suggest tectonic histories for the Tharsis region that are dependent on the relative age of the outer radial faults.

If Tharsis evolved from an isostatic state to flexurally supported loads as suggested by *Banerdt et al.* [1982] and by *Sleep and Phillips* [1985] (for their model in which the outer radial fractures are older than the central fractures), then the data presented here support the formation of the ridge system during the period of isostatic uplift. The observed ridge-fault crosscutting may have formed during the transition from a predominantly radially compressive to a dominantly tensile, circumferentially oriented stress regime. The orthogonal geometry and the relative ages of the ridge-fault crosscuts described by *Watters and Maxwell* [1983] could be explained by the formation of the radial fault system during and after the waning phase of the compressional ridge formation while maintaining the same general center of tectonic activity.

There are several problems with both of the models of *Banerdt et al.* [1982] and *Sleep and Phillips* [1985]. Neither model accounts for the observed deviation from the predicted, purely radially oriented, compressional stress field, demonstrated in the analysis of the symmetry of the inferred

compressive stresses (Figure 3). These deviations in ridge orientation are also responsible for the nonorthogonal ridge-fault crosscutting relations discussed by *Watters and Maxwell* [1983]. One important factor that may contribute to the differences between the predicted and inferred stresses is that both *Banerdt et al.* [1982] and *Sleep and Phillips* [1985] used a topographic and gravitational model only through the fourth harmonic, smoothing high-frequency variations. Use of higher-order harmonics, when better topography of Mars is available, could locally change the orientations and locations of the calculated stress trajectories (W. Banerdt, personal communication, 1985). Further, the present Tharsis topography was used to approximate the paleotopography, which could also account for some of the observed differences (W. Banerdt, personal communication, 1985).

In addition, the stresses calculated by *Banerdt et al.* [1982] and *Sleep and Phillips* [1985] are for the surface of a spherical lithosphere and stress must propagate to the free surface (lithosphere plus topography). This suggests that the ridges are the result of full lithospheric compression (i.e., deformation of the basement as well as the surface units). If this is the case and the ridges are a surface manifestation of basement reverse or thrust faults as *Plescia and Golombek* [1985] suggest, ridges might be expected to occur on exposed units of basement complex, adjacent to ridged plains, where they have not been observed (see Figure 5). *Watters and Maxwell* [1985*a*] suggest that the ridges are folds formed by thin-skinned deformation with little influence from the basement and that folding is a result of instability due to the viscosity contrast between the ridged plains units and the regolith substrate. A thin-skinned model is supported by recent studies of the ridges in the Yakima Fold Belt on Columbia Plateau of Washington State. The Columbia Plateau ridges are anticlinal folds formed in Miocene flood basalts that are morphologically and dimensionally similar to the ridges on the Tharsis Plateau and appear to have formed largely independent of the basement [*Watters and Maxwell*, 1985*b*]. If the ridges are the result of the type of folding envisioned by *Watters and Maxwell* [1985*a*], full lithospheric compression cannot be discounted.

Finally, stress trajectories for both isostatic models predict compression from roughly 40° to 110° (2400 to 6600 km) east of their stress centers. Ridges occur from as near as approximately 25° or 1500 km to only as far as about 70° or about 4200 km east of their centers. Compressional stress is predicted within 40° of their stress centers for both flexural loading models. However, *Banerdt et al.* [1982] calculate stresses between 80 and 160 MPa (800 and 1600 bars) resulting from flexural loading, much greater than the 10–30 MPa that they calculate from isostatic stresses. This raises a question as to what structural form will likely result from the predicted stresses. *Phillips and Lambeck* [1980] estimate the lower limit of the finite crustal strength of Mars to be between 30 and 50 MPa. *Banerdt and Golombek* [1985], using methods described by *Vink et al.* [1984], estimate that the total tensile and compressive yield strengths for the lithosphere of Mars are 1.2×10^{12} N/m and 3.3×10^{13} N/m, respectively, for a lithospheric thickness of 100 km, larger than the yield strength determined for terrestrial oceanic lithosphere. These total strengths are determined by integrating the lithospheric yield stress with depth curve, using Byerlee's law and appropriate flow laws to estimate yield stresses. If only the upper 1 km of the lithosphere is involved in the compressional deformation as suggested by *Watters and Maxwell* [1985*a*], the total crustal strength will, of course, be much smaller. In the upper crust, characterized by low temperatures and pressures, rock strength is controlled by frictional resistance to brittle failure [*Brace and Kohlstedt*, 1980]. Crustal strength in this brittle region is approximated by Byerlee's law:

$$\sigma_1 \simeq 5\,\sigma_3 \qquad \sigma_3 < 110 \text{ MPa}$$
$$\sigma_1 \simeq 3.1\,\sigma_3 + 210 \qquad \sigma_3 > 110 \text{ MPa}$$

expressed here in terms of maximum (σ_1) and minimum (σ_3) principal effective stresses [after *Brace and Kohlstedt*, 1980]. Applying Byerlee's law to the ridged plains units of Tharsis with an average thickness of 1 km [*DeHon*, 1981; *Saunders and Gregory*, 1980] and assuming $\rho = 2.9$ g/cm^3 (ρ of terrestrial basalt), the maximum tensile and compressive strength is approximately 10 and 40 MPa, respectively, at 1 km depth. This also assumes no pore fluid pressure (dry rock). Total yield strengths of the 1 km layer are 4×10^5 N/m tensile and 2×10^6 N/m compressive. Assuming that the magnitude and orientation of the principal stresses propogated from the surface of the lithosphere to the free surface are not significantly altered, the level of compressional stress predicted by *Banerdt et al.* [1982] for flexural loading would favor the formation of reverse or thrust faults within 40° of their stress center. The magnitude of compression predicted from isostatic stresses, however, favors the formation of folds beyond 40° of their stress center.

CONCLUSIONS

The Tharsis ridge system is roughly circumferential to the regional topographic high of northern Syria Planum and the major Tharsis volcanoes. Normals to vector means of ridge orientations indicate that the ridge system is not purely circumferentially oriented. Intersections of vector mean orientations plotted as great circles on a stereographic net shows the ridges are not concentric to a single point but to three broad zones. These observations indicate that either (1) the Tharsis ridge system did not form in response to a single regional compressional event with a single stress center but formed in response to a number of events with different centers, or (2) the majority of the Tharsis ridge system did form in response to a single event but with locally controlled deflections in the radially oriented stress field.

Compressional events that generated the ridges occurred after the emplacement of the ridged plains volcanic units (early in the Hesperian period) but before the episode of faulting that generated the majority of the observed ridge-fault crosscutting relationships on the ridged plains and the initial rifting of Valles Marineris. Compressional ridge formation did not continue beyond the emplacement of the Syria Planum Formation or the basal units of the Tharsis Montes Formation (during the latter half of the Hesperian period).

A reasonable correlation exists between the topographic edge of the Tharsis rise and outer extent of ridge occurrence. The outer extent of compressional deformation is about 5100 km from the regional topographic center located near northern Syria Planum. The innermost extent of compressional deformation cannot be determined because the ridged plains units have been buried by more recent volcanic units. However, ridge formation almost certainly extended farther

inward toward the topographic center than is presently observable.

The models of *Banerdt et al.* [1982] and *Sleep and Phillips* [1985], involving a combination of isostatic stresses and flexural loading, best explain the observed tensional features, topography, gravity, and, to a first approximation, the locations and orientations of the compressional ridges. If these models are correct, the formation of the compressional ridge system occurred during a period of isostatic uplift. The observed crosscutting of the ridges by faults may have formed during the transition from a predominantly compressive, radially oriented stress regime to a dominantly tensile, circumferentially oriented stress regime. The orthogonal geometry and relative ages of the ridge-fault intersections can be explained by the formation of the radial fault system during and after the waning phase of the compressional deformation that formed the ridges while maintaining the same general center of tectonic activity.

Acknowledgments. We thank George McGill, Jeff Plescia, Bruce Banerdt, and the Associate Editor for their reviews. We also wish to thank Steve Saunders, Don Wise, Baerbel Lucchitta, and George Stephens for useful discussions and comments on various aspects of the paper. We thank Donna Slattery for typing the manuscript and Rose Aiello for her help in preparing the figures. This research was supported by NASA grant NAGW-129.

REFERENCES

Balmino, G., B. Moynot, and N. Vales, Gravity field model of Mars in spherical harmonics up to degree and order eighteen, *J. Geophys. Res.*, *87*, 9735–9746, 1982.

Banerdt, W. B., and M. P. Golombek, Lithospheric strengths of the terrestrial planets (abstract), *Lunar Planet. Sci.*, *XVI*, 23–24, 1985.

Banerdt, W. B., R. J. Phillips, N. H. Sleep, and R. S. Saunders, Thick shell tectonics on one-plate planets: Applications to Mars, *J. Geophys. Res.*, *87*, 9723–9733, 1982.

Brace, W. F., and D. L. Kohlstedt, Limits on lithospheric stress imposed by laboratory experiments, *J. Geophys. Res.*, *85*, 6248–6252, 1980.

Carr, M. H., Volcanism on Mars, *J. Geophys. Res.*, *78*, 4049–4062, 1973.

Carr, M. H., Tectonism and volcanism of the Tharsis region of Mars, *J. Geophys. Res.*, *79*, 3943–3949, 1974.

DeHon, R. A., Thickness distribution of Tharsis volcanic materials (abstract), Reports of Planetary Geology Program, 1981, *NASA Tech. Memo*, *TM-84211*, 144–146, 1981.

Downs, G. S., P. J. Mouginis-Mark, S. H. Zisk, and T. W. Thompson, New radar-derived topography for the northern hemisphere of Mars, *J. Geophys. Res.*, *87*, 9747–9754, 1982.

Finnerty, A. A., and R. J. Phillips, A petrologic model for an isostatically compensated Tharsis region of Mars (abstract), paper presented at the 3rd International Colloquium on Mars, Lunar and Planet. Inst., Houston, Tex., 1981.

Golombek, M. P., and R. J. Phillips, Tharsis fault sequence as a test of a deformation mechanism (abstract), *Lunar Planet. Sci.*, *XIV*, 253–254, 1983.

Hartmann, W. K., Martian surface and crust: Review and synthesis, *Icarus*, *19*, 550–575, 1973.

Lucchitta, B. K., and J. L. Klockenbrink, Ridges and scarps in the equatorial belt of Mars, *Moon Planets*, *24*, 415–429, 1981.

Maxwell, T. A., Orientation and origin of ridges in the Lunae Planus—Coprates region of Mars, *Proc. Lunar Planet. Sci. Conf. 13th*, Part 1, *J. Geophys. Res.*, *87*, Suppl., A97–A108, 1982.

Phillips, R. J., and M. P. Golombek, Deformation sequence of Tharsis as a guide to thermal evolution (abstract), *Lunar Planet. Sci.*, *XIV*, 604–605, 1983.

Phillips, R. J., and K. Lambeck, Gravity fields of the terrestrial planets—Long-wavelength anomalies and tectonics, *Rev. Geophys.*, *18*, 27–76, 1980.

Phillips, R. J., and R. S. Saunders, The isostatic state of Martian topography, *J. Geophys. Res.*, *80*, 2893–2898, 1975.

Phillips, R. J., R. S. Saunders, and J. E. Conel, Mars: Crustal structure inferred from Bouguer gravity anomalies, *J. Geophys. Res.*, *78*, 4815–4820, 1973.

Plescia, J. B., and M. Golombeck, Origin of planetary wrinkle ridges from terrestrial analogs (abstract), *Lunar Planet. Sci.*, *XVI*, 667–668, 1985.

Plescia, J., and R. S. Saunders, Tectonics of the Tharsis region, Mars, *J. Geophys. Res.*, *87*, 9775–9791, 1982.

Reiche, P., An analysis of cross-lamination of the Coconino sandstone, *J. Geol.*, *44*, 905–932, 1938.

Roth, L. E., G. S. Downs, R. S. Saunders, and G. Schubert, Radar altimetry of south Tharsis, Mars, *Icarus*, *41*, 287–316, 1980.

Saunders, R. S., and T. E. Gregory, Tectonic implications of Martian ridged plains (abstract), Reports of Planetary Geology Program, 1980, *NASA Tech. Memo.*, *TM-82385*, 93–94, 1980.

Saunders, R. S., T. G. Bills, and L. Johansen, The ridged plains of Mars (abstract), *Lunar Planet. Sci.*, *XII*, 924–925, 1981.

Scott, D. H., Map showing lava flows in the southeast part of the Phoenicis Lacus quadrangle of Mars, *Misc. Invest. Map I-1274*, U.S. Geol. Surv., Reston, Va., 1981.

Scott, D. H., and M. H. Carr, Geologic map of Mars, *Misc. Invest. Map I-803*, U.S. Geol. Surv., Reston, Va., 1978.

Scott, D. H., and K. L. Tanaka, Preliminary geologic map of the western region of Mars, *Rep. OF 84-0659-A*, U.S. Geol. Surv., Denver, Colo., 1984.

Sleep, N. H., and R. J. Phillips, An isostatic model for the Tharsis province, Mars, *Geophys. Res. Lett.*, *6*, 803–806, 1979.

Sleep, N. H., and R. J. Phillips, Gravity and lithospheric stress on the terrestrial planets with reference to the Tharsis region of Mars, *J. Geophys. Res.*, *90*, 4469–4489, 1985.

Solomon, S. C., and J. W. Head, Evolution of the Tharsis province of Mars: The importance of heterogeneous lithospheric thickness and volcanic construction, *J. Geophys. Res.*, *87*, 9755–9774, 1982.

U.S. Geological Survey, Topographic map of Mars, scale 1:25,000,000, *Ser. M25M RMC*, *I-961*, Reston, Va., 1976.

Vink, G. E., W. J. Morgan, and W.-L. Zhao, Preferential rifting of continents: A source of displaced terrances, *J. Geophys. Res.*, *89*, 10,072–10,076, 1984.

Watters, T. R., and T. A. Maxwell, Crosscutting relations and relative ages of ridges and faults in the Tharsis region of Mars, *Icarus*, *56*, 278–298, 1983.

Watters, T. R., and T. A. Maxwell, Fold model for ridges of the Tharsis region of Mars (abstract), *Lunar Planet. Sci.*, *XVI*, 897–898, 1985*a*.

Watters, T. R., and T. A. Maxwell, Mechanisms of basalt-plains ridge formation (abstract), Reports of Planetary Geology Program, 1984, *NASA Tech. Memo.*, *TM-87563*, 479–481, 1985*b*.

Willemann, R. J., and D. L. Turcotte, The role of lithospheric stress in support of the Tharsis rise, *J. Geophys. Res.*, *87*, 9793–9801, 1982.

Wise, D. U., M. P. Golombek, and G. E. McGill, Tharsis province of Mars: Geologic sequence, geometry, and a deformation mechanism, *Icarus*, *38*, 458–472, 1979.

T. R. Watters and T. A. Maxwell, Center for Earth and Planetary Studies, National Air and Space Museum, Room 3101, Smithsonian Institution, Washington, DC 20560.

(Received July 30, 1985;
revised January 21, 1986;
accepted April 2, 1986.)